Available online at www.sciencedirect.com
ScienceDirect
Journal of Fluorine Chemistry 128 (2007) 404–412
JOURNAL OF FLUORINE CHEMISTRY
www.elsevier.com/locate/fluor

Review

Hydrogen bonded H_3O^+, H_2O, HF, F^- in fluoride metalates (Al, Cr, Fe, Zr, Ta) templated with *tren* (tris-(2-aminoethyl)amine)

Karim Adil [a], Mohamed Ali Saada [a], Amor Ben Ali [a], Monique Body [b], Minh Trung Dang [a], Annie Hémon-Ribaud [a], Marc Leblanc [a], Vincent Maisonneuve [a,*]

[a] *Laboratoire des Oxydes et Fluorures, UMR CNRS 6010, IRIM2F, FR-2575 CNRS, Faculté des Sciences et Techniques, Université du Maine, Avenue Olivier Messiaen, 72085 Le Mans Cedex 09, France*
[b] *Laboratoire de Physique de l'Etat Condensé, UMR CNRS 6087, IRIM2F, FR-2575 CNRS, Faculté des Sciences et Techniques, Université du Maine, Avenue Olivier Messiaen, 72085 Le Mans Cedex 09, France*

Received 19 September 2006; received in revised form 20 October 2006; accepted 25 October 2006
Available online 2 November 2006

Abstract

The environment of H_3O^+, H_2O, HF and F^- species (non-bonded to metals) is considered in fluoride metalates which crystallise from the $(Al(OH)_3$, $Cr(OH)_3$, FeF_3, ZrF_4, $Ta_2O_5)$-*tren*-$HF_{aq.}$–ethanol systems (microwave heating at 190 °C during 1 h). The presence of $(H_3O)(H_2O)_6^+$ clusters or H_3O^+ cations, of isolated or associated H_2O molecules, of $(HF_2)^-$ and F^- anions is evidenced. The thermal stability of the solids depends strongly on the nature of the hydrogen-bonded species associated with the preceding cations or anions and on the formation of water ribbons or layers.
© 2006 Elsevier B.V. All rights reserved.

Keywords: Hybrid fluorides; Hydrothermal synthesis; Microwave heating; Hydrogen bond; Water cluster

Contents

1. Introduction

Numerous fluorides crystallise when *tren* amine (tris-(2-aminoethyl)amine) reacts with metal oxides, hydroxides or fluorides and aqueous HF in solvothermal conditions at low temperature [1–8]. According to the $HF_{aq.}$ content, the amine is tri- or tetra-protonated and the corresponding $[H_3tren]^{3+}$ or $[H_4tren]^{4+}$ cations counterbalance the anionic charge of the fluorinated inorganic subnetwork. Most often, the metal (oxide)fluoride species, which result from the condensation of MX_n units ($X = F^-$, O^{2-}, OH^-, OH_2), are isolated and few compounds exhibit extended 1D chains. Inorganic 2D or 3D open structures are still unknown with *tren* template.

It is frequently observed that extra cations (H_3O^+), molecules (H_2O, HF) or anions (F^-) are hydrogen bonded with the preceding amine cations and fluoride (poly)anions; as expected, their presence is strongly correlated with the HF content of the starting solution. The environment of these

* Corresponding author. Tel.: +33 2 4383 3561; fax: +33 2 4383 3506.
E-mail address: vincent.maisonneuve@univ-lemans.fr (V. Maisonneuve).

0022-1139/$ – see front matter © 2006 Elsevier B.V. All rights reserved.
doi:10.1016/j.jfluchem.2006.10.015

associated entities is discussed in the article, together with the thermal stability of the solids. Aluminium Al^{III} or 3d metal fluorides (Fe^{III}, Cr^{III}) and 4d metal fluorides (Zr^{IV}, Ta^{V}) are considered.

2. Results and discussion

More than 18 crystalline phases are found in the $Al(OH)_3$–*tren*–$HF_{aq.}$–EtOH system at 190 °C ($t = 1$ h, microwave heating) [9]. The formation domains, which depend on the aluminium, amine and HF contents, undergo a strong evolution in the composition space diagram, illustrated in Fig. 1 for $[Al^{3+}] = 0.1$ mol L^{-1}. The geometric symbols, associated with the composition of the solids, are located at the figurative points of the starting compositions. Several of the 18 solids have very narrow formation domains ($(H_3O)\cdot[H_4tren]_2\cdot(Al_7F_{30})$ or $[H_3tren]_4\cdot(Al_2F_{11})(AlF_6)_2\cdot(F)\cdot 10H_2O$) and mixtures are frequently encountered. The ZrF_4–*tren*–$HF_{aq.}$–EtOH system [10] exhibits only 8 formation domains for $[Zr^{4+}] = 0.5$ mol L^{-1} (Fig. 1) whereas the Ta_2O_5–*tren*–$HF_{aq.}$–EtOH system is even more simple for $[Ta^{V}] = 0.2$ mol L^{-1} (Fig. 1). Few starting compositions were tested in the FeF_3-*tren*-$HF_{aq.}$-EtOH [11] or $Cr(OH)_3$–*tren*–$HF_{aq.}$–EtOH [12] systems.

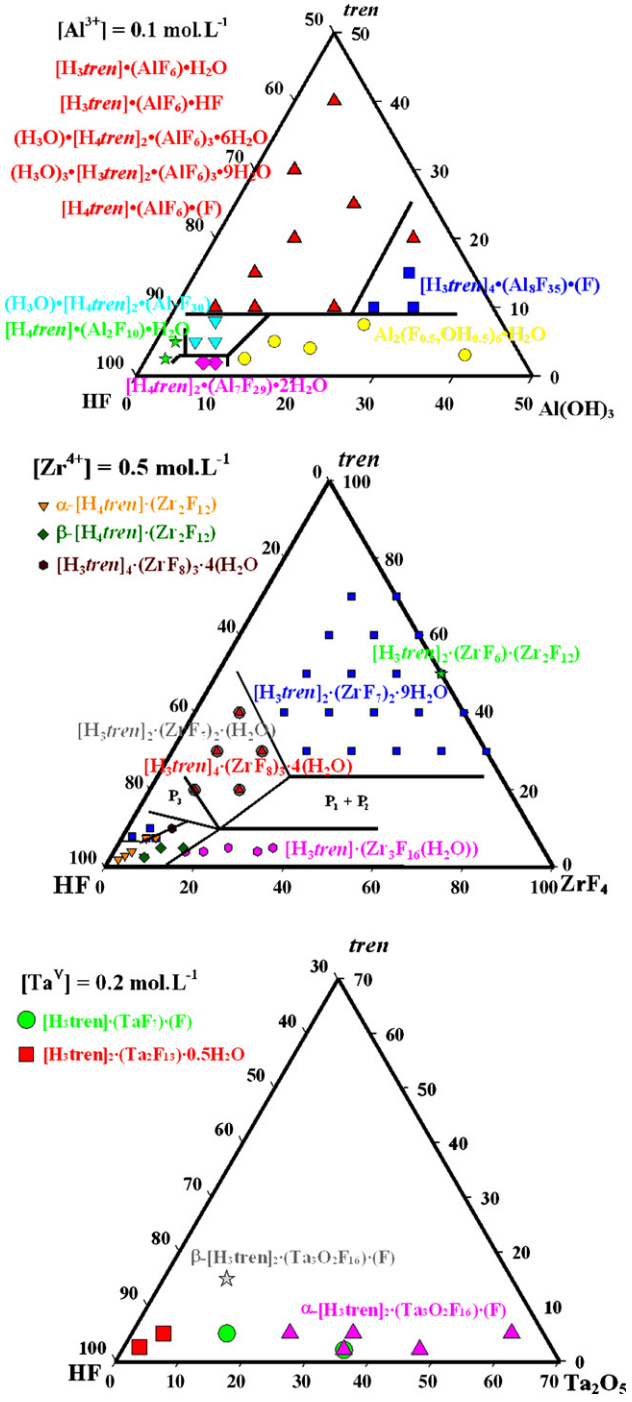

Fig. 1. Composition space of the ($Al(OH)_3$, ZrF_4, Ta_2O_5)–*tren*–$HF_{aq.}$–ethanol systems at 190 °C.

The evolution of the formulations of the crystalline solids is compatible with the variation of the starting mixture compositions: the $[H_4tren]^{4+}$ cations appear only at high HF concentration while the solids are built up from isolated MX_n species at high amine concentration. A condensation of the MX_n anions occurs at low amine concentration in order to give extended polyanions: corner sharing or edge sharing MX_n polyhedra build dimers, tetramers, heptamers or octamers and infinite chains. Such entities are illustrated in Fig. 2. Al^{3+}, Cr^{3+}, Fe^{3+} cations are always six-fold coordinated while Zr^{IV} and Ta^{V} adopt six-, seven- or eight-fold coordinations.

It is now demonstrated that geometrical considerations are indicative of the protonation state of the amine (Fig. 3): a "spider" shape with N_p–N_t–N_p angles smaller than ≈95° or larger than ≈100° and a "scorpion" shape with two (or three) N_p–N_t distances shorter than ≈3.2 Å or longer than ≈3.3 Å are significant of $[H_3tren]^{3+}$ and $[H_4tren]^{4+}$ cations, respectively. A "planar" configuration occurs for $[H_4tren]^{4+}$ cations.

3. Environment of H_3O^+ cations

H_3O^+ cations are found in $(H_3O)\cdot[H_4tren]_2\cdot(Al_7F_{30})$ and $(H_3O)\cdot[H_4tren]_2\cdot(AlF_6)_3\cdot 6H_2O$. In $(H_3O)\cdot[H_4tren]_2\cdot(Al_7F_{30})$, hydronium cations adopt a distorted octahedral coordination (Fig. 4 top left). Six fluoride anions of two (Al_7F_{30}) polyanions lie at the average distance $\langle d_{O\cdots F}\rangle = 2.89$ Å (Table 1). The (Al_7F_{30}) units and H_3O^+ cations build infinite chains along the [1 1 1] direction of the triclinic cell. In $(H_3O)\cdot[H_4tren]_2\cdot(AlF_6)_3\cdot 6H_2O$, hydronium cations are supposed to be surrounded by three water molecules, $O_W(1)$, $O_W(3)$, $O_W(5)$, at the average distance $\langle d_{O\cdots O}\rangle = 2.88$ Å, by three fluoride ions, F(8), F(9), F(10), at $\langle d_{O\cdots F}\rangle = 3.11$ Å and by three water molecules $O_W(2)$, $O_W(4)$, $O_W(6)$, at longer distances $\langle d_{O\cdots O}\rangle = 3.21$ Å (Fig. 4 top right and bottom left). Nine extra fluoride anions are hydrogen bonded with water molecules. Consequently, the $(H_3O)\cdot(H_2O)_6^+$ cluster is surrounded by twelve fluoride anions of eight AlF_6 octahedra (Fig. 4 bottom right). Water molecules build a distorted octahedron. Such a geometry is not reminiscent of any of 14 *ab initio* optimised configurations of protonated water clusters $(H)\cdot(H_2O)_7^+$, assumed to exist as H_3O^+ centered $[H_3O^+(H_2O)_6]$ or $H_5O_2^+$ centered $[H_5O_2^+(H_2O)_5]$ species [13]; none of two possible cagelike forms is octahedral.

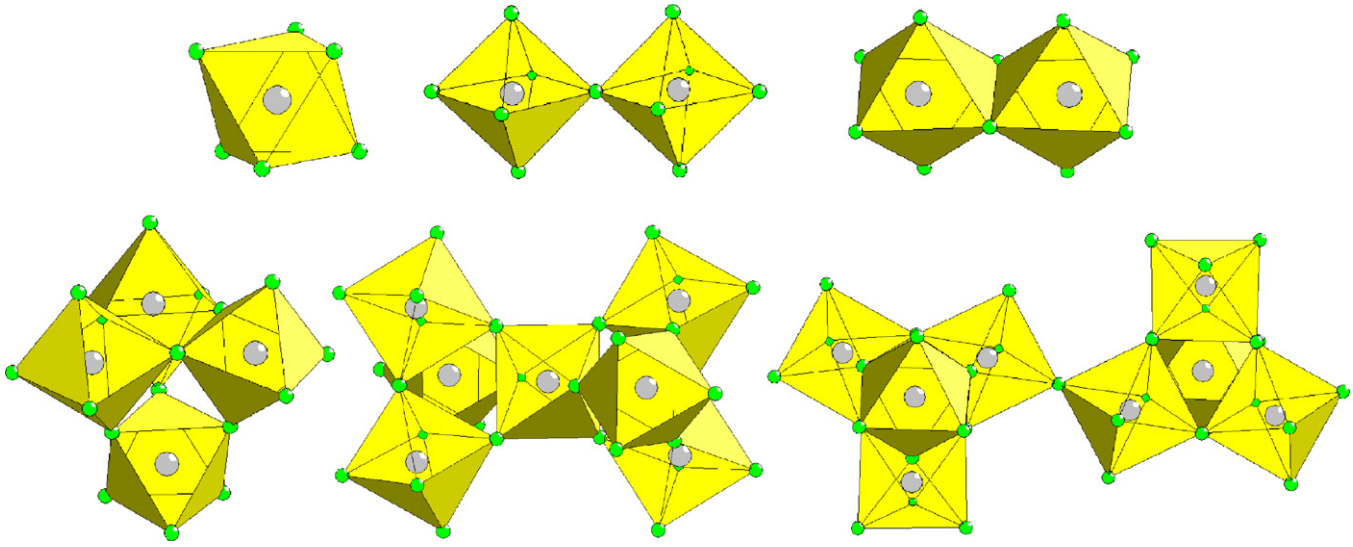

Fig. 2. Extended polyanions derived from AlF_6 units (top left): Al_2F_{11} (middle top), Al_2F_{10} (top right), Al_4F_{18} (bottom left), Al_7F_{30} (bottom middle) and Al_8F_{35} (bottom right).

4. Environment of H_2O molecules

Numerous hydrates exist in fluoride metalates (Table 2). Water molecules are isolated at low hydration degree of the solids while their association into infinite layers becomes effective at high hydration degree. It must be noted that $[H_3tren]_2{\cdot}(ZrF_7)_2{\cdot}9H_2O$ presents isolated and associated water molecules simultaneously. The structure of $[H_3tren]_2{\cdot}(AlF_5(H_2O))_3{\cdot}8H_2O$ is not yet accurately described and seems to exhibit infinite ribbons of water molecules and, curiously, a disorder between two water molecules and one fluoride ion in 6c sites appears in $[H_3tren]{\cdot}[H_4tren]{\cdot}(Al_4F_{18}){\cdot}(F,2H_2O)$.

Isolated water molecules adopt frequently a triangular coordination by two fluoride anions and one $–NH_3^+$ cation (Table 2). A tendency to build infinite chains of inorganic (poly)anions and water molecules surrounded by organic cations can be noted in $[H_3tren]{\cdot}(AlF_6){\cdot}H_2O$ (Fig. 5 top left) and $[H_4tren]{\cdot}(Al_2F_{10}){\cdot}H_2O$ (Fig. 5 top right). In this last phase, two water molecules are associated with two fluoride ions of two Al_2F_{10} units. A similar configuration is found in $[H_4tren]{\cdot}(TaF_7)_2{\cdot}H_2O$; however the hydrogen bonds are bifurcated and a five-fold coordination is implied (Fig. 5 bottom left). Octahedral coordination occurs only with $–NH_3^+$ cations (Table 2); the $O_w\cdots N$ distances are close to the mean distance observed for $–NH_3^+\cdots O_w$ distances, 2.84 Å [14]. It can be supposed that coordination of water molecules by two fluoride anions and one $–NH_3^+$ cation is not very stable: the thermal decomposition of $[H_4tren]{\cdot}(TaF_7)_2{\cdot}H_2O$, $[H_4tren]_2{\cdot}(Al_7F_{29}){\cdot}2H_2O$ and $[H_3tren]$-

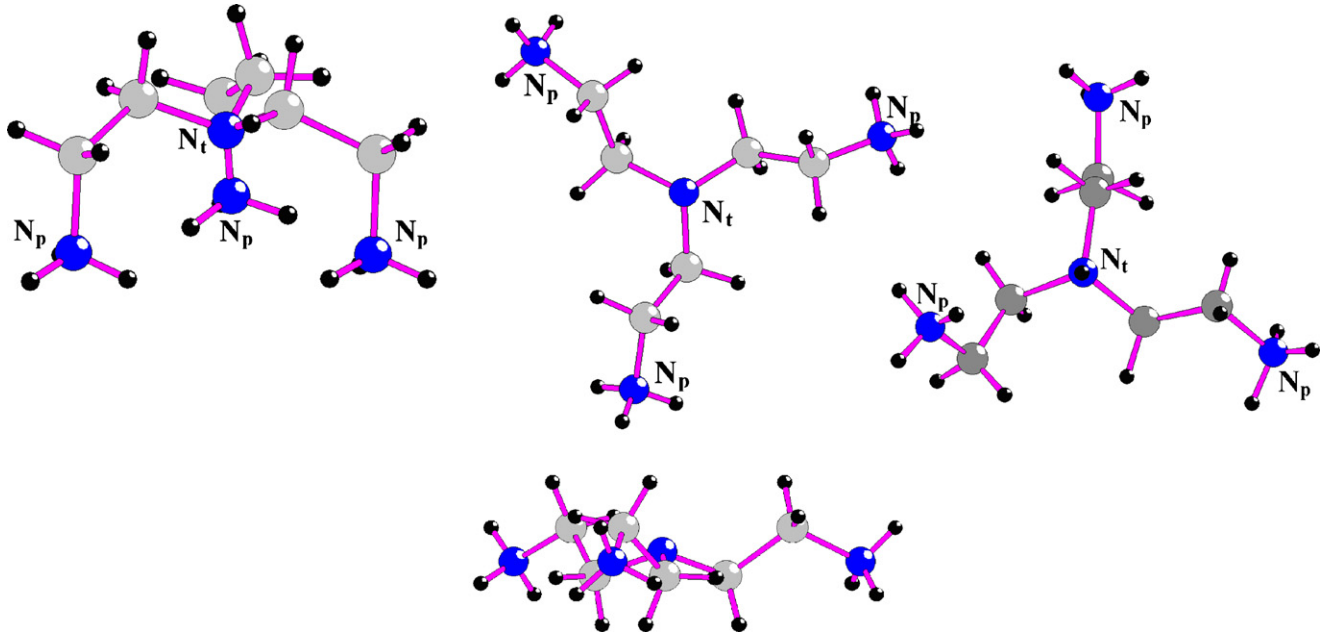

Fig. 3. "Spider" (left), "planar" (middle), "scorpion" (right) configurations of the $[H_3tren]^{3+}$ and $[H_4tren]^{4+}$ cations.

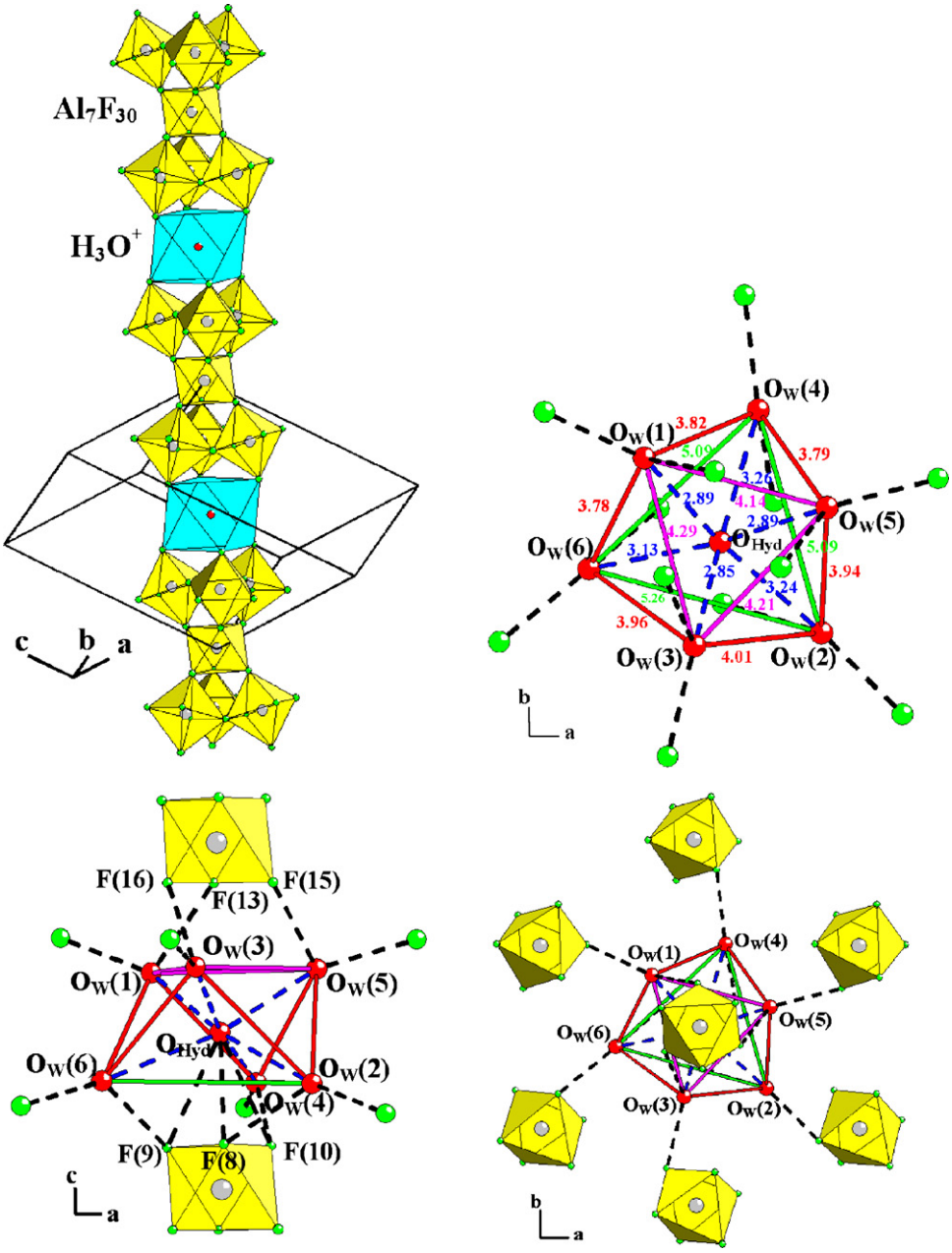

Fig. 4. Environment of H_3O^+ cations in $(H_3O)\cdot[H_4tren]_2\cdot(Al_7F_{30})$ (top left) and $[(H_3O)\cdot(H_2O)_6]^+$ cluster in $(H_3O)\cdot[H_4tren]_2\cdot(AlF_6)_3\cdot 6H_2O$.

$\cdot[H_4tren]\cdot(Al_4F_{18})\cdot(F,2H_2O)$ starts at room temperature with the loss of these water molecules. The stability is strongly reinforced by the presence of Al_2F_{10} dimers and by chain formation in $[H_4tren]\cdot(Al_2F_{10})\cdot H_2O$: decomposition occurs at $T \approx 190$ °C.

When water molecules associate into infinite layers, they are inserted between neutral sheets of interacting organic cations and fluoride polyanions; then, it is expected that thermal stability is weak. Such a behaviour is clearly demonstrated by thermal analysis and X-ray diffractometry in $[H_3tren]_2\cdot(ZrF_7)_2\cdot 9H_2O$. Water molecules are located into three different crystallographic sites of *R*32 space group, 3a, 6c, 18f. Water molecules in 3a are octahedrally surrounded by six $-NH_3^+$ groups of two amine cations (Fig. 5 bottom right). Water molecules in 6c ($O_w(2)$) and 18f ($O_w(3)$) build infinite water layers (Fig. 6 top right and Table 3) which outgas at 60–90 °C, probably in two consecutive steps: $O_w(3)$ at ≈60 °C and $O_w(2)$ at ≈90 °C. The dehydration reactions are reversible and topotactic; they leave unchanged the stable $[H_3tren]_2\cdot(ZrF_7)_2\cdot H_2O$ sheets. Above 210 °C, the decomposition of $[H_3tren]_2\cdot(ZrF_7)_2\cdot H_2O$ occurs and the reaction is irreversible. The overall evolution scheme is:

$$[H_3tren]_2\cdot(ZrF_7)_2\cdot 9H_2O \xrightarrow[(\approx 60\,^\circ C)]{-6H_2O} [H_3tren]_2\cdot(ZrF_7)_2\cdot 3H_2O \xrightarrow[(\approx 90\,^\circ C)]{-2H_2O} [H_3tren]_2\cdot(ZrF_7)_2\cdot H_2O$$

$$3/2[H_3tren]_2\cdot(ZrF_7)_2\cdot H_2O \xrightarrow[(\approx 285\,^\circ C)]{-(3/2H_2O+[H_3tren]F_3)} [H_3tren]_2\cdot(ZrF_6)\cdot(Zr_2F_{12})$$

Table 1
Selected $H_3O^+\cdots X$ (X = O_w of H_2O, F^-) and $H_2O\cdots X$ distances (X = O_{Hyd} of H_3O^+, F^-) in $(H_3O)\cdot[H_4tren]_2\cdot(Al_7F_{30})$ and $(H_3O)\cdot[H_4tren]_2\cdot(AlF_6)_3\cdot 6H_2O$

$(H_3O)\cdot[H_4tren]_2\cdot(Al_7F_{30})$			H_3O^+
X			6F
Geometry			Octahedral
$\langle d_{O\cdots F}\rangle$			2.89
$(H_3O)\cdot[H_4tren]_2\cdot(AlF_6)_3\cdot 6H_2O$	X	$\langle d_{O\cdots F}\rangle$	$\langle d_{O\cdots O}\rangle$
H_3O^+ in $(H_3O)(H_2O)_6^+$ cluster			
O_{Hyd}	$(3+3)O_w + 3F$	3.11	2.88 + 3.21
H_2O in $(H_3O)(H_2O)_6^+$ cluster			
$O_w(1)$	$O_{Hyd} + 2F$	2.62	2.89
$O_w(3)$	$O_{Hyd} + 2F$	2.62	2.85
$O_w(5)$	$O_{Hyd} + 2F$	2.64	2.89
$O_w(2)$	$O_{Hyd} + 2F$	2.65	3.24
$O_w(4)$	$O_{Hyd} + 2F$	2.59	3.26
$O_w(6)$	$O_{Hyd} + 2F$	2.60	3.13

Water layers adopt a trigonal symmetry in $[H_3tren]_2\cdot(ZrF_7)_2\cdot 9H_2O$ and $[H_3tren]_4\cdot(Al_2F_{11})(AlF_6)_2\cdot(F)\cdot 10H_2O$. In $[H_3tren]_2\cdot(ZrF_7)_2\cdot 9H_2O$, the hexagonal cycles are corrugated and similar to that found in ice Ih, Ic or III. In $[H_3tren]_4\cdot(Al_2F_{11})(AlF_6)_2\cdot(F)\cdot 10H_2O$, the cycles involve twelve water molecules (Fig. 6 bottom right). Six corners of one cycle are common to three $(H_2O)_{12}$ cycles and these positions are decorated with the AlF_6 and Al_2F_{11} units. Five crystallographic sites describe the water molecule positions. Hydrogen bonds are clearly established in the $(H_2O)_{12}$ cycles and with fluoride ions which lie above or below the mean plane of water molecules. Only one over five water molecules ($O_W(4)$) adopts a tetrahedral coordination (Table 3). In $[H_3tren]_2\cdot(FeF_3(H_2O)_3)(FeF_6)_2\cdot 8H_2O$, the hydration water molecules build infinite layers of corrugated squares and nonagons (Fig. 6 bottom left). Metal bonded water molecules are also found and one of these water molecules is disordered with one fluoride ion in a neutral distorted octahedron.

Table 2
Selected $A\cdots X$ distances in fluoride metalates (A = H_2O, HF, F^-; X = N of $-NH_3^+$, F^-)

A = H_2O	X	Geometry	$\langle d_{O\cdots F}\rangle$	$\langle d_{O\cdots N}\rangle$
$[H_3tren]\cdot(AlF_6)\cdot H_2O$	2F + N	Triangular	2.64	2.74
$[H_3tren]\cdot[H_4tren]\cdot(Al_4F_{18})\cdot(F,2H_2O)$	2F + N	Triangular	2.97	3.09
$[H_4tren]\cdot(Al_2F_{10})\cdot H_2O$	2F + N	Triangular	2.68	2.69
$[H_4tren]_2\cdot(Al_7F_{29})\cdot 2H_2O$	2F + N	Triangular	2.84	2.82
$[H_4tren]\cdot(TaF_7)_2\cdot H_2O$	4F + N	Prismatic	3.01	2.97
$[H_3tren]_4\cdot(ZrF_8)_3\cdot 4H_2O$	3N	Triangular		3×2.73
$[H_3tren]_6\cdot(TaOF_6)_4(ZrF_7)_2\cdot 3H_2O$	6N	Octahedral		6×2.87
$[H_3tren]_2\cdot(ZrF_7)_2\cdot 9H_2O$ $O_w(1)$	6N	Octahedral		6×2.87

A = HF	X	$d_{F\cdots F}$
$[H_3tren]\cdot(AlF_6)\cdot HF$	1F	2.38
$[H_3tren]\cdot(CrF_6)\cdot HF$	1F	2.44

A = F^-	X	Geometry	$\langle d_{F\cdots N}\rangle$
$[H_4tren]\cdot(AlF_6)\cdot(F)$	3N	Triangular	2.67
$[H_4tren]\cdot(FeF_6)\cdot(F)$	3N	Triangular	2.67
$[H_3tren]\cdot(TaF_7)\cdot(F)$	5N	Pyramidal	2.77
α-$[H_3tren]_2\cdot(Ta_3O_2F_{16})\cdot(F)$	6N	Octahedral	2.86
β-$[H_3tren]_2\cdot(Ta_3O_2F_{16})\cdot(F)$	6N	Octahedral	2.84
$[H_3tren]_4\cdot(Al_2F_{11})(AlF_6)_2\cdot(F)\cdot 10H_2O$	6N	Octahedral	2.81

Table 3
Selected $H_2O\cdots X$ distances in water layers of fluoride metalates (X = O_w of H_2O, F^-)

H_2O layers	A	X	Geometry	$\langle d_{O\cdots F}\rangle$	$\langle d_{O\cdots O}\rangle$
$[H_3tren]_2\cdot(ZrF_7)_2\cdot 9H_2O$	$O_w(2)$	$3O_w$	Triangular		2.81
	$O_w(3)$	$3O_w + F$	Tetrahedral	2.83	2.82
$[H_3tren]_4\cdot(Al_2F_{11})(AlF_6)_2\cdot(F)\cdot 10H_2O$	$O_w(2)$	$3O_w$	Triangular		2.78
	$O_w(1)$	$2O_w + F$	Triangular	2.73	2.77
	$O_w(3)$	$2O_w + F$	Triangular	2.69	2.74
	$O_w(5)$	$2O_w + F$	Triangular	2.81	2.83
	$O_w(4)$	$3O_w + F$	Tetrahedral	2.67	2.78
$[H_3tren]_2\cdot(FeF_3(H_2O)_3)(FeF_6)_2\cdot 8H_2O$	$O_w(2)$	$2O_w + F$	Triangular	2.71	2.81
	$O_w(3)$	$2O_w + 2F$	Tetrahedral	2.94	2.84
	$O_w(1)$	$4O_w$	Tetrahedral		2.83
	$O_w(4)$	$3O_w + F$	Tetrahedral	2.59	2.58

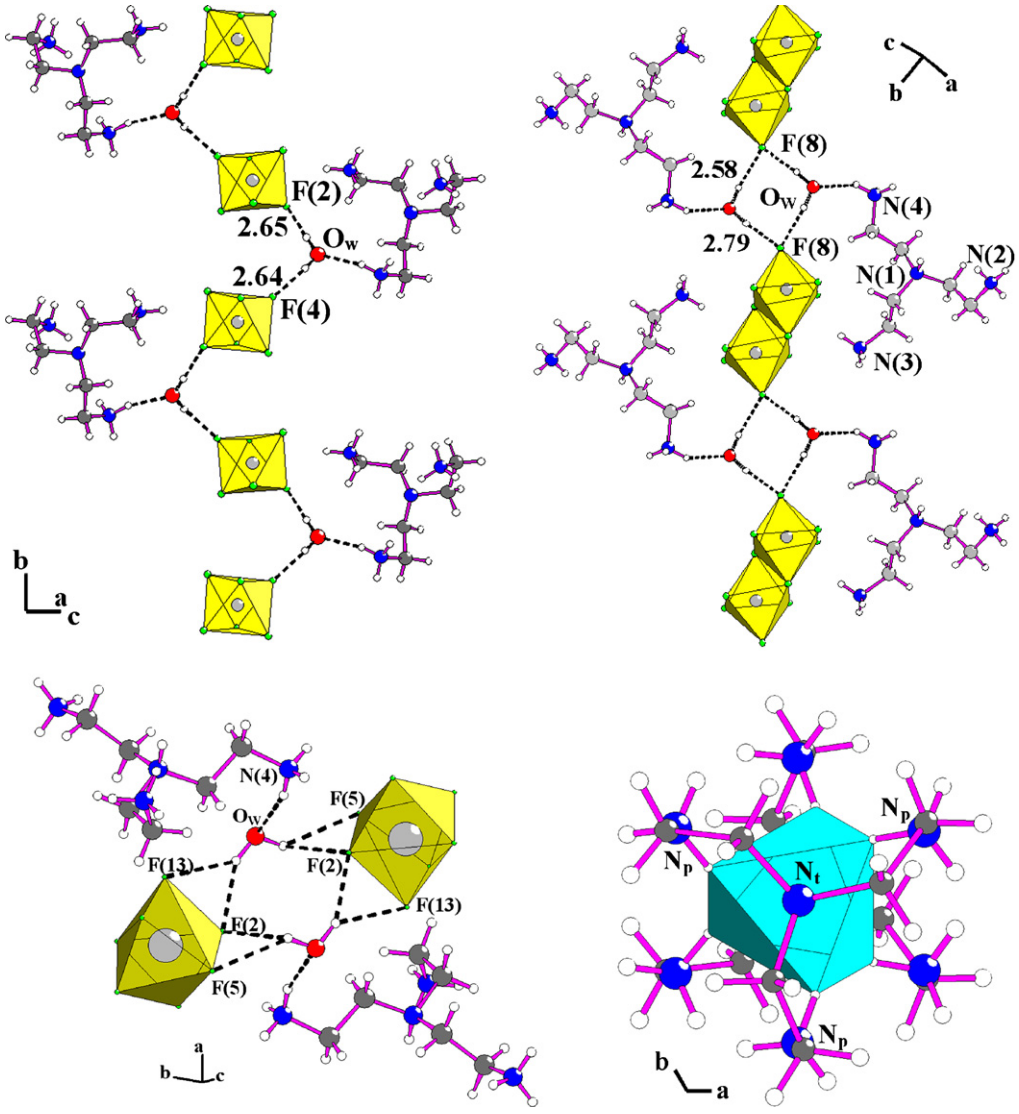

Fig. 5. Environment of H_2O molecules in $[H_3tren]\cdot(AlF_6)\cdot H_2O$ (top left), $[H_4tren]\cdot(Al_2F_{10})\cdot H_2O$ (top right), $[H_4tren]\cdot(TaF_7)_2\cdot H_2O$ (bottom left) and octahedral coordination of $O_w(1)$ water molecules in $[H_3tren]\cdot(ZrF_7)\cdot 9H_2O$ (bottom right).

In $[H_3tren]_2\cdot(AlF_5(H_2O))_3\cdot 8H_2O$, one water molecule is coordinated with Al^{3+}. In spite of the poor quality of the structure determination, branched chains of edge-sharing hexagons can be recognized. The resulting infinite ribbons of water molecules are connected with $[H_3tren]^{3+}$ cations and $(AlF_5(H_2O))^{2-}$ units (Fig. 6 top left and Table 4). Thermal decomposition of $[H_3tren]_2\cdot(AlF_5(H_2O))_3\cdot 8H_2O$ starts at ≈40 °C and ends at ≈180 °C with the loss of 11 water molecules per formula unit and the formation of an amorphous phase. Then, recrystallisation occurs at $T \approx 200$ °C and is followed by a phase transformation or decomposition at $T \approx 240$ °C. Both new crystalline phases are still unknown.

It must be noted that pentagons and octagons of water molecules are not encountered in fluoride metalates while they are frequently found in clathrates [15,16], in organic crystals [17] or in ice structures [18].

5. Environment of HF molecules

Short F···F distances between one fluoride anion of $(AlF_6)^{3-}$ or $(CrF_6)^{3-}$ units and a free fluorine atom, 2.38 and 2.44 Å, are observed in $[H_3tren]\cdot(AlF_6)\cdot HF$ (Fig. 7) and isostructural $[H_3tren]\cdot(CrF_6)\cdot HF$, respectively (Table 2). They suggest the presence of a strongly hydrogen bonded HF molecule and the existence of the $(HF_2)^-$ anion. The corresponding Al–F or Cr–F distance, 1.819(3) or 1.903(3) Å, respectively, is not affected by the formation of this bond (the average Al–F and Cr–F distances are 1.80 and 1.90 Å, respectively). It must be noted that the next nearest neighbours of HF, five hydrogen atoms of five $–CH_2$ groups, are located at much longer distances, 2.46–2.77 Å; if any, the associated hydrogen bonds are very weak. The thermal decomposition of $[H_3tren]\cdot(CrF_6)\cdot HF$ starts at ≈40 °C and ends at ≈100 °C.

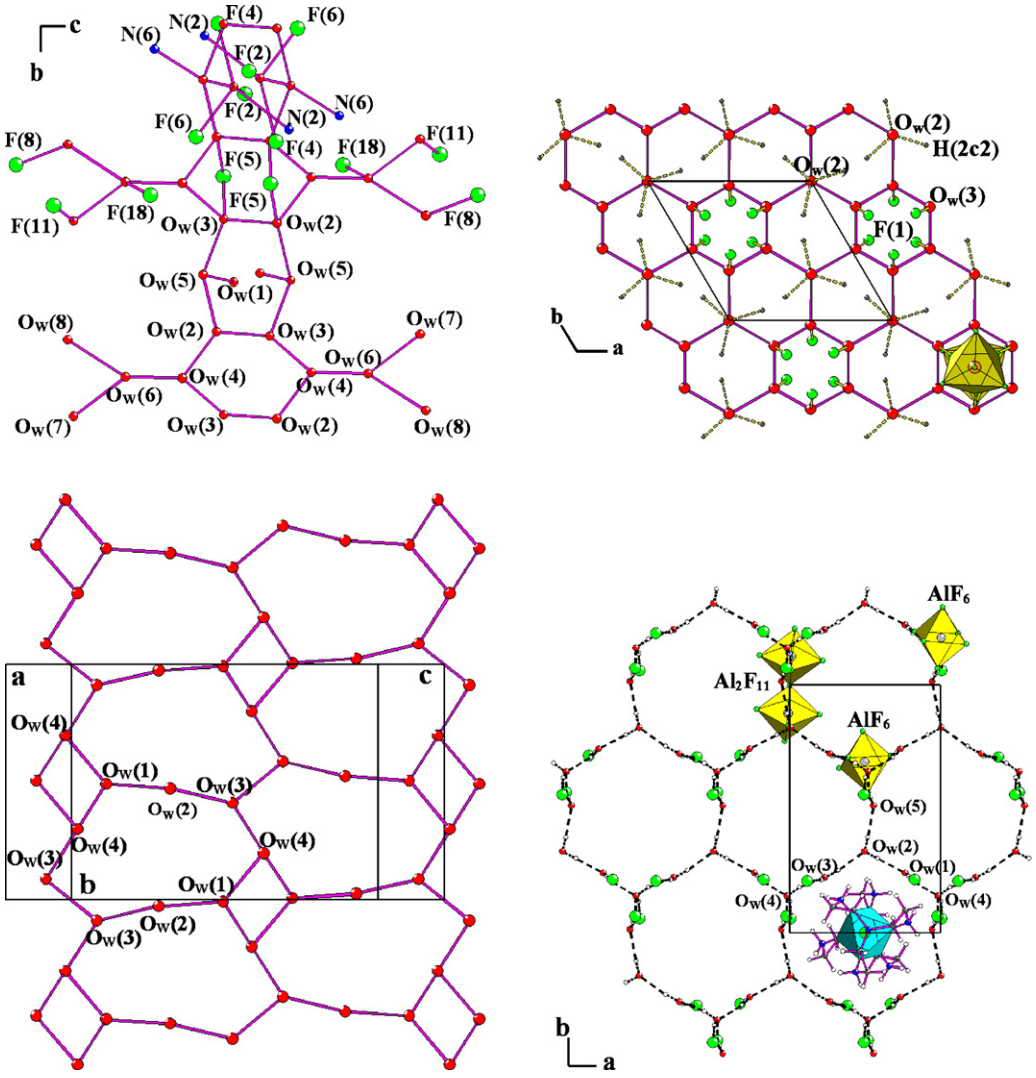

Fig. 6. Water ribbon in $[H_3tren]_2{\cdot}(AlF_5(H_2O))_3{\cdot}8H_2O$ (top left) and water layers in $[H_3tren]{\cdot}(ZrF_7){\cdot}9H_2O$ (top right), $[H_3tren]_2{\cdot}(FeF_3(H_2O)_3)(FeF_6)_2{\cdot}8H_2O$ (bottom left) and $[H_3tren]_4{\cdot}(Al_2F_{11})(AlF_6)_2{\cdot}(F){\cdot}10H_2O$ (bottom right).

NMR experiments were performed in order to ascertain the nature of the ''HF'' species in $[H_3tren]{\cdot}(AlF_6){\cdot}HF$ [19]. The ^{19}F NMR spectrum of $[H_3tren]{\cdot}(AlF_6){\cdot}HF$ is given in Fig. 8. The aluminium bonded fluoride ions in six 4e sites ($P2_1/c$ space group) are responsible of the intense signals at $\delta_{iso.} \approx 15$–35 ppm; these chemical shift values are very similar to the values observed in the series of related fluorides $[H_3N(CH_2)_xNH_3]{\cdot}AlF_5$ ($x = 6$, 8, 10 and 12) [20]. The smaller signal at $\delta_{iso.} \approx 92$ ppm is attributed to the F(7) species (in 4e site) of $(HF_2)^-$ anions.

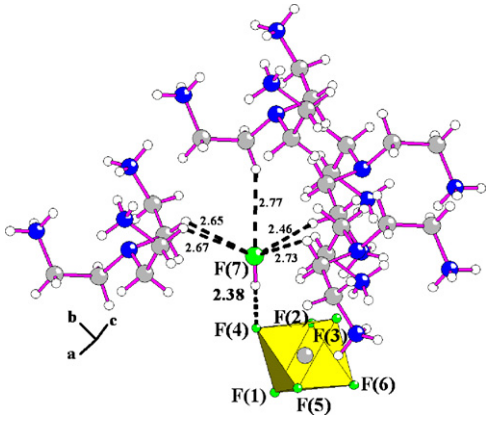

Fig. 7. Environment of $(HF_2)^-$ anion in $[H_3tren]{\cdot}(AlF_6){\cdot}HF$.

Table 4
Selected $H_2O\cdots X$ distances in water ribbons of $[H_3tren]_2{\cdot}(AlF_5(H_2O))_3{\cdot}8H_2O$ ($X = O_w$ of H_2O, F^-)

H_2O	X	Geometry	$\langle d_{O\cdots F}\rangle$	$\langle d_{O\cdots O}\rangle$	$\langle d_{O\cdots N}\rangle$
H_2O ribbon					
$O_w(1)$	N + 3F	Tetrahedral	2.77		3.07
$O_w(2)$	$3O_w$ + F	Tetrahedral	2.63	2.80	
$O_w(3)$	$3O_w$ + F	Tetrahedral	2.70	2.77	
$O_w(4)$	$3O_w$	Triangular		2.78	
$O_w(5)$	$3O_w$ + N	Tetrahedral		2.89	2.86
$O_w(6)$	$3O_w$ + F	Tetrahedral	2.66	2.87	
$O_w(7)$	O_w + F	Angular	2.69	2.86	
$O_w(8)$	O_w + F	Angular	2.83	3.00	

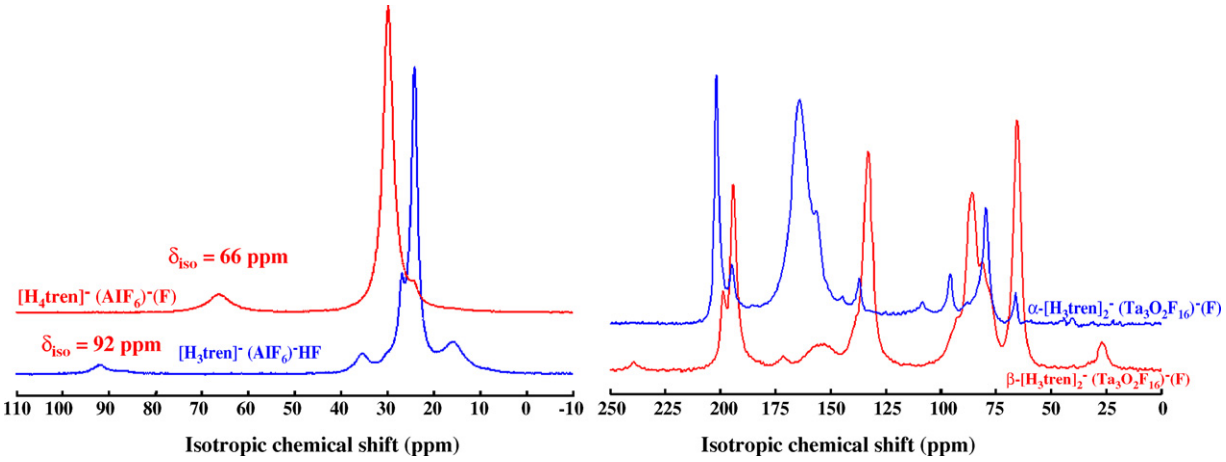

Fig. 8. ^{19}F NMR patterns of [H_3tren]·(AlF_6)·HF, [H_4tren]·(AlF_6)·(F) (left), α-[H_3tren]$_2$·($Ta_3O_2F_{16}$)·(F) and β-[H_3tren]$_2$·($Ta_3O_2F_{16}$)·(F) (right) (the external reference, choosen for isotropic chemical shift determination, is C_6F_6 ($\delta_{iso.}(C_6F_6)$ vs. $CFCl_3$ = − 164.2 ppm [29]).

The F···F distances in the $(HF_2)^-$ anions are slightly longer than F···F distances observed in KHF_2 (2.26 Å) [21], $BaHF_3$ (2.27 Å) [22], $Ba_5Nb_3O_3F_{18}(HF_2)$ (2.21 Å) [23] or in (1-ethyl-3-methyl)imidazolium difluoride (2.21 Å) [24].

6. Environment of F^- anions

Non-metal bonded fluoride ions (''free'' fluoride ions) are always surrounded by $–NH_3^+$ groups in fluoride metalates (Table 2). Similarly to water molecules, their coordination is comprised between three (triangular) and six (octahedral). The F···N distances increase with the coordination number; this variation of hydrogen bond lengths is well known [25].

In [H_4tren]·(AlF_6)·(F), ''free'' fluoride ions F(3) adopt a triangular coordination; the N–H···F angle is 168.7(5)° and the H···F distance is 1.79(2) Å (Fig. 9 top). Three hydrogen atoms H(2D) of three $–CH_2$ groups are located at much longer distances ($d_{H\cdots F}$ = 2.57(2) Å and $d_{C\cdots F}$ = 3.46(2) Å).

In [H_3tren]$_4$·(Al_2F_{11})(AlF_6)$_2$·(F)·10H_2O, ''free'' fluoride ion F(13) is located at the center of an octahedron of six $–NH_3^+$ groups of two $[H_3tren]^{3+}$ cations (Fig. 9 bottom right). This F[H_3tren]$_2$ assembly projects at the vertical of the center of $(H_2O)_{12}$ cycles (Fig. 6 bottom right). A similar octahedral

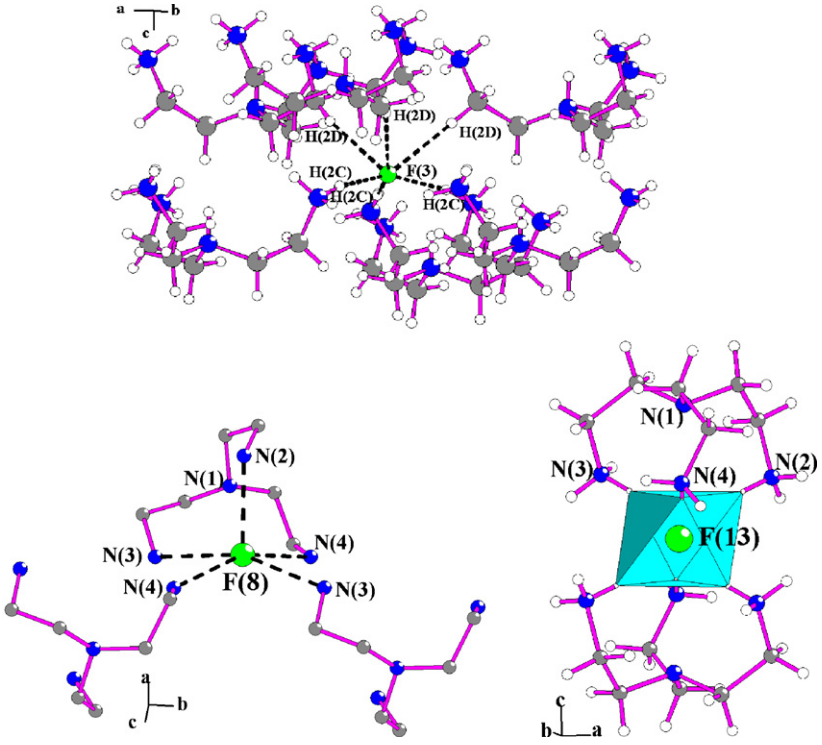

Fig. 9. Triangular, pyramidal and octahedral environments of fluoride ions in [H_4tren]·(AlF_6)·(F) (top), [H_3tren](TaF_7)·(F) (bottom left) and [H_3tren]$_4$·(Al_2F_{11})(AlF_6)$_2$·(F)·10H_2O (bottom right), respectively.

coordination is found in α-$[H_3tren]_2\cdot(Ta_3O_2F_{16})\cdot(F)$ and β-$[H_3tren]_2\cdot(Ta_3O_2F_{16})\cdot(F)$. In these last phases, a disorder affects the positions of tantalum bonded fluoride ions of $Ta_3O_2F_{16}$ trimers.

A square pyramidal geometry, derived from the preceding octahedral geometry, describes the environment of ''free'' fluoride ion F(8) in $[H_3tren]\cdot(TaF_7)\cdot(F)$ (Fig. 9 bottom left).

The ^{19}F NMR spectra of $[H_4tren]\cdot(AlF_6)\cdot(F)$, α-$[H_3tren]_2\cdot(Ta_3O_2F_{16})\cdot(F)$ and β-$[H_3tren]_2\cdot(Ta_3O_2F_{16})\cdot(F)$ are given in Fig. 8. In $[H_4tren]\cdot(AlF_6)\cdot(F)$, the aluminium bonded fluoride ions in two 6c sites ($P6_3$ space group) correspond to the intense peak at $\delta_{iso.} \approx 30$ ppm. The small peak at $\delta_{iso.} \approx 66$ ppm can be associated to a non-metal bonded fluoride ion: F(3) in 2a sites (Fig. 8 left). Such ''free'' fluoride ions, with similar chemical shifts, were already described in other fluorides $[H_3N(CH_2)_6NH_3]_2\cdot(M(OH,F)_6)\cdot(OH,F)\cdot H_2O$ (M = Al and In) [26], in D4R units [27] or in ULM-5 [28]. In α-$[H_3tren]_2\cdot(Ta_3O_2F_{16})\cdot(F)$ and β-$[H_3tren]_2\cdot(Ta_3O_2F_{16})\cdot(F)$, the disordered environment of metal bonded fluoride ions implies numerous geometrical configurations of the linear trimer built up from two $TaOF_6$ polyhedra trans-linked with a central TaO_2F_4 octahedron. The chemical shift range expands from ≈20 to ≈200 ppm and the signal from ''free'' fluoride ions cannot be distinguished from the signals of metal bonded fluoride ions (Fig. 8 right).

7. Conclusion

Until now, the dimensionality of fluoride metalates templated with *tren* amine cations is limited to 1D; no 3D microporous fluoride has been obtained. However, large unknown polyanions are now available (with Al^{3+}). It can be supposed that a further step to the condensation of these polyanions consists in the thermal treatment of suitable starting materials.

It is demonstrated that intermediate phases appear during the controlled heating of several hydrated aluminates or zirconates; their *ab initio* structure determinations must be performed. However, the evolution of these transient phases is strongly dependent on the local partial pressures of H_2O or HF vapours, which surround the solids.

It is clear that the octahedral association of H_2O and six $-NH_3^+$ cations is quite stable. At the opposite, the presence of water layers or ribbons decreases strongly the thermal stability of all the investigated fluorides.

Acknowledgements

Thanks are due to the Région des Pays de Loire for a post-doctoral fellowship (A.B.A.), to the Institut Français de Coopération (Tunis) for a doctorate grant (M.A.S.) and to the Agence Universitaire pour la Francophonie (Hanoï) (M.T.D.).

References

[1] E. Goreshnik, M. Leblanc, V. Maisonneuve, Z. Anorg. Allg. Chem. 628 (2002) 162–166.
[2] J. Pinkas, H.W. Roesky, J. Fluor. Chem. 122 (2003) 125–150.
[3] E. Goreshnik, M. Leblanc, V. Maisonneuve, J. Solid State Chem. 177 (2004) 4023–4030.
[4] K. Adil, M. Leblanc, V. Maisonneuve, Acta Crystallogr. E60 (2004) m1379–m1381.
[5] K. Adil, A. Ben Ali, G. Dujardin, R. Dhal, M. Leblanc, V. Maisonneuve, J. Fluor. Chem. 125 (2004) 1709–1714.
[6] M. Ali Saada, A. Hémon-Ribaud, M. Leblanc, V. Maisonneuve, J. Fluor. Chem. 126 (2005) 1072–1077.
[7] M. Ali Saada, A. Hémon-Ribaud, L.S. Smiri, M. Leblanc, V. Maisonneuve, J. Fluor. Chem. 126 (2005) 1246–1251.
[8] K. Adil, A. Ben Ali, M. Leblanc, V. Maisonneuve, Solid State Sci. 8 (2006) 698–703.
[9] K. Adil, M. Leblanc, V. Maisonneuve, J. Am. Chem. Soc., submitted for publication.
[10] M. Ali Saada, A. Hémon-Ribaud, M. Leblanc, V. Maisonneuve, Solid State Sci., submitted for publication.
[11] A. Ben Ali, J.M. Grenèche, M. Leblanc, V. Maisonneuve, J. Solid State Chem., submitted for publication.
[12] M. T. Dang, A. Hémon-Ribaud, M. Leblanc, V. Maisonneuve, Acta Crystallogr., submitted for publication.
[13] J.-C. Jiang, Y.-S. Wang, H.-C. Chang, S.H. Lin, Y.T. Lee, G. Niedner-Schatteburg, H.-C. Chang, J. Am. Chem. Soc. 122 (2000) 1398–1410.
[14] T. Steiner, Angew. Chem. Int. Ed. 41 (2002) 48–76.
[15] R. Ludwig, Angew. Chem. 113 (2001) 1856–1876.
[16] R. Ludwig, Angew. Chem. Int. Ed. 40 (2001) 1809–1827.
[17] N.S. Oxtoby, A.J. Blake, N.R. Champness, C. Wilson, Chem. Eur. J. 11 (2005) 4643–4654.
[18] C. Lobban, J.L. Finney, W.F. Kuhs, Nature 391 (1998) 268–270.
[19] M. Body, J.Y. Buzaré, K. Adil, V. Maisonneuve, submitted for publication.
[20] E. Goreshnik, M. Leblanc, E. Gaudin, F. Taulelle, V. Maisonneuve, Solid State Sci. 4 (2002) 1213–1219.
[21] J.A. Ibers, J. Phys. 25 (1964) 474–477.
[22] W. Massa, E. Herdtweck, Acta Crystallogr. C 39 (1983) 509–512.
[23] M.P. Crosnier-Lopez, H. Duroy, J.L. Fourquet, J. Solid State Chem. 107 (1993) 211–217.
[24] K. Matsumoto, T. Tsuda, R. Hagiwara, Y. Ito, O. Tamada, Solid State Sci. 4 (2002) 23–26.
[25] T. Steiner, Acta Crystallogr. B 54 (1998) 456–463.
[26] J. Touret, X. Bourdon, M. Leblanc, R. Retoux, J. Renaudin, V. Maisonneuve, J. Fluor. Chem. 110 (2001) 133–138.
[27] P. Reinert, J. Patarin, T. Loiseau, G. Férey, H. Kessler, Micropor. Mesopor. Mater. 22 (1998) 43–55.
[28] T. Loiseau, D. Riou, F. Taulelle, G. Férey, Zeolites Rel. Micropor. Mater. 84 (1994) 395–402.
[29] B. Bureau, G. Silly, J. Emery, J.-Y. Buzaré, Chem. Phys. 249 (1999) 89–104.